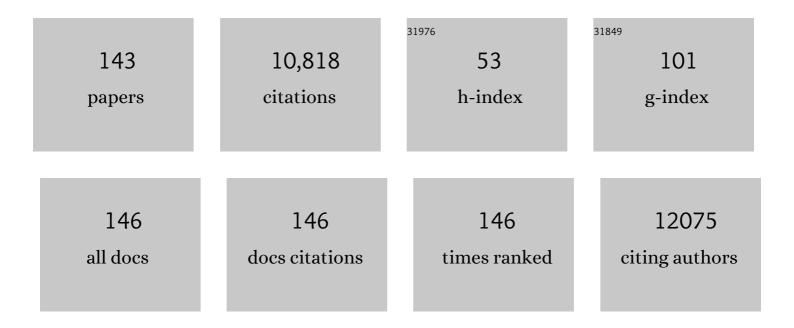
Sam M Webb

List of Publications by Year in descending order

Source: https://exaly.com/author-pdf/7749682/publications.pdf Version: 2024-02-01



SAM M WERR

#	Article	IF	CITATIONS
1	Reexamination of 2.5-Ga "whiff―of oxygen interval points to anoxic ocean before GOE. Science Advances, 2022, 8, eabj7190.	10.3	42
2	X-ray Fluorescence Spectroscopy of Picrolite Raw Material on Cyprus. Heritage, 2022, 5, 664-677.	1.9	1
3	X-ray fluorescence microscopy methods for biological tissues. Metallomics, 2022, 14, .	2.4	19
4	Trace Impurities Identified as Forensic Signatures in CMX-5 Fuel Pellets Using X-ray Spectroscopic Techniques. Analytical Chemistry, 2022, 94, 7084-7091.	6.5	4
5	Synchrotron xâ€ray fluorescence analysis reveals diagenetic alteration of fossil melanosome trace metal chemistry. Palaeontology, 2021, 64, 63-73.	2.2	2
6	Iron Heterogeneity in Early Active Multiple Sclerosis Lesions. Annals of Neurology, 2021, 89, 498-510.	5.3	22
7	Microbial sulfate reduction and organic sulfur formation in sinking marine particles. Science, 2021, 371, 178-181.	12.6	64
8	Electrochemically induced metal- <i>vs.</i> ligand-based redox changes in mackinawite: identification of a Fe ³⁺ - and polysulfide-containing intermediate. Dalton Transactions, 2021, 50, 11763-11774.	3.3	6
9	Organic sulfur fluxes and geomorphic control of sulfur isotope ratios in rivers. Earth and Planetary Science Letters, 2021, 562, 116838.	4.4	9
10	Changing chemistry of particulate manganese in the near- and far-field hydrothermal plumes from 15°S East Pacific Rise and its influence on metal scavenging. Geochimica Et Cosmochimica Acta, 2021, 300, 95-118.	3.9	10
11	An ecophysiological explanation for manganese enrichment in rock varnish. Proceedings of the National Academy of Sciences of the United States of America, 2021, 118, .	7.1	19
12	Manganese oxides in Martian meteorites Northwest Africa (NWA) 7034 and 7533. Icarus, 2021, 364, 114471.	2.5	8
13	Rapid, Concurrent Formation of Organic Sulfur and Iron Sulfides During Experimental Sulfurization of Sinking Marine Particles. Global Biogeochemical Cycles, 2021, 35, e2021GB007062.	4.9	10
14	Brachiopod δ34SCAS microanalyses indicate a dynamic, climate-influenced Permo-Carboniferous sulfur cycle. Earth and Planetary Science Letters, 2020, 546, 116428.	4.4	11
15	Arsenolipids in Cultured Picocystis Strain ML and Their Occurrence in Biota and Sediment from Mono Lake, California. Life, 2020, 10, 93.	2.4	20
16	Reinforcement Learning for Adaptive Illumination with X-rays. , 2020, , .		6
17	Investigation of the effect of taurine supplementation on muscle taurine content in the mdx mouse model of Duchenne muscular dystrophy using chemically specific synchrotron imaging. Analyst, The, 2020, 145, 7242-7251.	3.5	7
18	Sample preparation with sucrose cryoprotection dramatically alters Zn distribution in the rodent hippocampus, as revealed by elemental mapping. Journal of Analytical Atomic Spectrometry, 2020, 35, 2498-2508.	3.0	19

#	Article	IF	CITATIONS
19	Seasonal Zinc Storage and a Strategy for Its Use in Buds of Fruit Trees. Plant Physiology, 2020, 183, 1200-1212.	4.8	12
20	Robust framework and software implementation for fast speciation mapping. Journal of Synchrotron Radiation, 2020, 27, 1049-1058.	2.4	9
21	Hierarchical biota-level and taxonomic controls on the chemistry of fossil melanosomes revealed using synchrotron X-ray fluorescence. Scientific Reports, 2020, 10, 8970.	3.3	9
22	Deposition of sulfate aerosols with positive Δ33S in the Neoarchean. Geochimica Et Cosmochimica Acta, 2020, 285, 1-20.	3.9	4
23	Sulfur isotope fractionation between aqueous and carbonate-associated sulfate in abiotic calcite and aragonite. Geochimica Et Cosmochimica Acta, 2020, 280, 317-339.	3.9	28
24	Efficient phloem remobilization of Zn protects apple trees during the early stages of Zn deficiency. Plant, Cell and Environment, 2019, 42, 3167-3181.	5.7	18
25	Chemical and Isotopic Evidence for Organic Matter Sulfurization in Redox Gradients Around Mangrove Roots. Frontiers in Earth Science, 2019, 7, .	1.8	15
26	Fate of cobalt and nickel in mackinawite during diagenetic pyrite formation. American Mineralogist, 2019, 104, 917-928.	1.9	16
27	The source of sulfate in brachiopod calcite: Insights from μ-XRF imaging and XANES spectroscopy. Chemical Geology, 2019, 529, 119328.	3.3	10
28	Synchrotron X-ray absorption spectroscopy of melanosomes in vertebrates and cephalopods: implications for the affinity of <i>Tullimonstrum</i> . Proceedings of the Royal Society B: Biological Sciences, 2019, 286, 20191649.	2.6	16
29	Tissue-specific geometry and chemistry of modern and fossilized melanosomes reveal internal anatomy of extinct vertebrates. Proceedings of the National Academy of Sciences of the United States of America, 2019, 116, 17880-17889.	7.1	32
30	Depositional and diagenetic constraints on the abundance and spatial variability of carbonate-associated sulfate. Chemical Geology, 2019, 523, 59-72.	3.3	23
31	Fe-bearing phases in modern lacustrine microbialites from Mexico. Geochimica Et Cosmochimica Acta, 2019, 253, 201-230.	3.9	11
32	Insights Into the Mineralogy and Surface Chemistry of Extracellular Biogenic SO Globules Produced by Chlorobaculum tepidum. Frontiers in Microbiology, 2019, 10, 271.	3.5	29
33	Midâ€Proterozoic Ferruginous Conditions Reflect Postdepositional Processes. Geophysical Research Letters, 2019, 46, 3114-3123.	4.0	7
34	Photons, Folios, and Fossils: The X-ray Imaging and Spectroscopy Program of Ancient Materials at SSRL. Synchrotron Radiation News, 2019, 32, 22-28.	0.8	4
35	Biogenesis of zinc storage granules in <i>Drosophila melanogaster</i> . Journal of Experimental Biology, 2018, 221, .	1.7	28
36	Periphyton and abiotic factors influencing arsenic speciation in aquatic environments. Environmental Toxicology and Chemistry, 2018, 37, 903-913.	4.3	9

#	Article	IF	CITATIONS
37	Insights into the Interconnection of the Electrodes and Electrolyte Species in Lithium–Sulfur Batteries Using Spatially Resolved <i>Operando</i> X-ray Absorption Spectroscopy and X-ray Fluorescence Mapping. Journal of Physical Chemistry C, 2018, 122, 5303-5316.	3.1	10
38	From lapis lazuli to ultramarine blue: investigating Cennino Cennini's recipe using sulfur K-edge XANES. Pure and Applied Chemistry, 2018, 90, 463-475.	1.9	31
39	Molecular genetic and biochemical characterization of a putative family of zinc metalloproteins in Caenorhabditis elegans. Metallomics, 2018, 10, 1814-1823.	2.4	2
40	Coupled X-ray Fluorescence and X-ray Absorption Spectroscopy for Microscale Imaging and Identification of Sulfur Species within Tissues and Skeletons of Scleractinian Corals. Analytical Chemistry, 2018, 90, 12559-12566.	6.5	14
41	Redox Fluctuations and Organic Complexation Govern Uranium Redistribution from U(IV)-Phosphate Minerals in a Mining-Polluted Wetland Soil, Brittany, France. Environmental Science & Technology, 2018, 52, 13099-13109.	10.0	40
42	A new synchrotron rapid-scanning X-ray fluorescence (SRS-XRF) imaging station at SSRL beamline 6-2. Journal of Synchrotron Radiation, 2018, 25, 1565-1573.	2.4	19
43	Organic carbon burial during OAE2 driven by changes in the locus of organic matter sulfurization. Nature Communications, 2018, 9, 3409.	12.8	62
44	Cold crucible induction melter test for crystalline ceramic waste form fabrication: A feasibility assessment. Journal of Nuclear Materials, 2017, 486, 283-297.	2.7	21
45	Pathogenic implications of distinct patterns of iron and zinc in chronic MS lesions. Acta Neuropathologica, 2017, 134, 45-64.	7.7	94
46	Biomineralization of U(VI) phosphate promoted by microbially-mediated phytate hydrolysis in contaminated soils. Geochimica Et Cosmochimica Acta, 2017, 197, 27-42.	3.9	26
47	Quantifying Cr(VI) Production and Export from Serpentine Soil of the California Coast Range. Environmental Science & Technology, 2017, 51, 141-149.	10.0	58
48	Evidence for the Root-Uptake of Arsenite at Lateral Root Junctions and Root Apices in Rice (Oryza) Tj ETQq0 0 0	rgBT/Ove 1.0	rlock 10 Tf 50
49	Iron mineralogy and redox conditions during deposition of the mid-Proterozoic Appekunny Formation, Belt Supergroup, Glacier National Park. Special Paper of the Geological Society of America, 2016, , 221-242.	0.5	8
50	Deletion of Phytochelatin Synthase Modulates the Metal Accumulation Pattern of Cadmium Exposed C. elegans. International Journal of Molecular Sciences, 2016, 17, 257.	4.1	15
51	MP19-17 SPATIAL DISTRIBUTION AND CONCENTRATION OF ELEMENTS WITHIN LIESEGANG-LIKE RINGS IN APATITE-BASED KIDNEY STONES. Journal of Urology, 2016, 195, .	0.4	0
52	Nutrient and pollutant metals within earthworm residues are immobilized in soil during decomposition. Soil Biology and Biochemistry, 2016, 101, 217-225.	8.8	8
53	The chemical, mechanical, and hydrological evolution of weathering granitoid. Journal of Geophysical Research F: Earth Surface, 2016, 121, 1410-1435.	2.8	49
54	Relating structure and composition with accessibility of a single catalyst particle using correlative	12.8	74

3-dimensional micro-spectroscopy. Nature Communications, 2016, 7, 12634.

#	Article	IF	CITATIONS
55	Real-Time Manganese Phase Dynamics during Biological and Abiotic Manganese Oxide Reduction. Environmental Science & Technology, 2016, 50, 4248-4258.	10.0	69
56	Copper Speciation in Variably Toxic Sediments at the Ely Copper Mine, Vermont, United States. Environmental Science & Technology, 2016, 50, 1126-1136.	10.0	7
57	Manganese mineralogy and diagenesis in the sedimentary rock record. Geochimica Et Cosmochimica Acta, 2016, 173, 210-231.	3.9	150
58	Sulfur K-edge XANES of lazurite: Toward determining the provenance of lapis lazuli. Microchemical Journal, 2016, 125, 299-307.	4.5	26
59	Microbial- and thiosulfate-mediated dissolution of mercury sulfide minerals and transformation to gaseous mercury. Frontiers in Microbiology, 2015, 6, 596.	3.5	17
60	Mineral Density Volume Gradients in Normal and Diseased Human Tissues. PLoS ONE, 2015, 10, e0121611.	2.5	57
61	Zinc Speciation in Contaminated Sediments: Quantitative Determination of Zinc Coordination by X-ray Absorption Spectroscopy. Aquatic Geochemistry, 2015, 21, 295-312.	1.3	10
62	Speciation Matters: Bioavailability of Silver and Silver Sulfide Nanoparticles to Alfalfa (<i>Medicago) Tj ETQq0 0</i>	0 rgBT/Ov	erlgçk 10 Tf
63	Multiscale Speciation of U and Pu at Chernobyl, Hanford, Los Alamos, McGuire AFB, Mayak, and Rocky Flats. Environmental Science & Technology, 2015, 49, 6474-6484.	10.0	43
64	Strain-guided mineralization in the bone–PDL–cementum complex of a rat periodontium. Bone Reports, 2015, 3, 20-31.	0.4	16
65	Sedimentary iron–phosphorus cycling under contrasting redox conditions in a eutrophic estuary. Chemical Geology, 2015, 392, 19-31.	3.3	55
66	Spatial imaging of Zn and other elements in Huanglongbing-affected grapefruit by synchrotron-based micro X-ray fluorescence investigation. Journal of Experimental Botany, 2014, 65, 953-964.	4.8	42
67	Neoarchean carbonate–associated sulfate records positive Δ ³³ S anomalies. Science, 2014, 346, 739-741.	12.6	70
68	Leaf metallome preserved over 50 million years. Metallomics, 2014, 6, 774-782.	2.4	35
69	Chromium(<scp>iii</scp>) oxidation by biogenic manganese oxides with varying structural ripening. Environmental Sciences: Processes and Impacts, 2014, 16, 2127-2136.	3.5	61
70	The narwhal (<i>Monodon monoceros</i>) cementum–dentin junction: A functionally graded biointerphase. Proceedings of the Institution of Mechanical Engineers, Part H: Journal of Engineering in Medicine, 2014, 228, 754-767.	1.8	6
71	Microbiological Reduction of Sb(V) in Anoxic Freshwater Sediments. Environmental Science & Technology, 2014, 48, 218-226.	10.0	108
72	Constraints on Precipitation of the Ferrous Arsenite Solid H ₇ Fe ₄ (AsO ₃) ₅ . Journal of Environmental Quality, 2014, 43, 947-954.	2.0	7

#	Article	IF	CITATIONS
73	Elastic discontinuity due to ectopic calcification in a human fibrous joint. Acta Biomaterialia, 2013, 9, 4787-4795.	8.3	7
74	Distributed microbially- and chemically-mediated redox processes controlling arsenic dynamics within Mn-/Fe-oxide constructed aggregates. Geochimica Et Cosmochimica Acta, 2013, 104, 29-41.	3.9	41
75	Manganese-oxidizing photosynthesis before the rise of cyanobacteria. Proceedings of the National Academy of Sciences of the United States of America, 2013, 110, 11238-11243.	7.1	189
76	Reply to Jones and Crowe: Correcting mistaken views of sedimentary geology, Mn-oxidation rates, and molecular clocks. Proceedings of the National Academy of Sciences of the United States of America, 2013, 110, E4119-20.	7.1	8
77	Efficient xylem transport and phloem remobilization of <scp>Z</scp> n in the hyperaccumulator plant species <i><scp>S</scp>edum alfredii</i> . New Phytologist, 2013, 198, 721-731.	7.3	106
78	The plastic nature of the human bone–periodontal ligament–tooth fibrous joint. Bone, 2013, 57, 455-467.	2.9	44
79	Mercury Localization and Speciation in Plants Grown Hydroponically or in a Natural Environment. Environmental Science & Technology, 2013, 47, 3082-3090.	10.0	80
80	In Situ X-ray Absorption Spectroscopy Investigation of a Bifunctional Manganese Oxide Catalyst with High Activity for Electrochemical Water Oxidation and Oxygen Reduction. Journal of the American Chemical Society, 2013, 135, 8525-8534.	13.7	478
81	Uranium(VI) Interactions with Mackinawite in the Presence and Absence of Bicarbonate and Oxygen. Environmental Science & Technology, 2013, 47, 7357-7364.	10.0	44
82	Micro x-ray absorption spectroscopic analysis of arsenic localization and biotransformation in Chironomus riparius Meigen (Diptera: Chironomidae) and Culex tarsalis Coquillett (Culicidae). Environmental Pollution, 2013, 180, 78-83.	7.5	16
83	(Micro)spectroscopic Analyses of Particle Size Dependence on Arsenic Distribution and Speciation in Mine Wastes. Environmental Science & Technology, 2013, 47, 8164-8171.	10.0	40
84	The role of anaerobic respiration in the immobilization of uranium through biomineralization of phosphate minerals. Geochimica Et Cosmochimica Acta, 2013, 106, 344-363.	3.9	57
85	Uranium redox transition pathways in acetate-amended sediments. Proceedings of the National Academy of Sciences of the United States of America, 2013, 110, 4506-4511.	7.1	161
86	Brine film thicknesses on mica surfaces under geologic CO ₂ sequestration conditions and controlled capillary pressures. Water Resources Research, 2013, 49, 5071-5076.	4.2	15
87	Melanin Concentration Gradients in Modern and Fossil Feathers. PLoS ONE, 2013, 8, e59451.	2.5	39
88	Mn(II) oxidation by an ascomycete fungus is linked to superoxide production during asexual reproduction. Proceedings of the National Academy of Sciences of the United States of America, 2012, 109, 12621-12625.	7.1	178
89	Geochemical Weathering Increases Lead Bioaccessibility in Semi-Arid Mine Tailings. Environmental Science & Technology, 2012, 46, 5834-5841.	10.0	48
90	Imaging of stroke: a comparison between X-ray fluorescence and magnetic resonance imaging methods. Magnetic Resonance Imaging, 2012, 30, 1416-1423.	1.8	15

#	Article	IF	CITATIONS
91	Imaging translocation and transformation of bioavailable selenium by Stanleya pinnata with X-ray microscopy. Analytical and Bioanalytical Chemistry, 2012, 404, 1277-1285.	3.7	7
92	Arsenic and chromium speciation in an urban contaminated soil. Chemosphere, 2012, 88, 1196-1201.	8.2	55
93	Microscale Imaging and Identification of Fe Speciation and Distribution during Fluid–Mineral Reactions under Highly Reducing Conditions. Environmental Science & Technology, 2011, 45, 4468-4474.	10.0	65
94	Changes in Zinc Speciation with Mine Tailings Acidification in a Semiarid Weathering Environment. Environmental Science & Technology, 2011, 45, 7166-7172.	10.0	19
95	Diversity of Mn oxides produced by Mn(II)-oxidizing fungi. Geochimica Et Cosmochimica Acta, 2011, 75, 2762-2776.	3.9	161
96	Defining the distribution of arsenic species and plant nutrients in rice (Oryza sativa L.) from the root to the grain. Geochimica Et Cosmochimica Acta, 2011, 75, 6655-6671.	3.9	75
97	The effect of pH and natural microbial phosphatase activity on the speciation of uranium in subsurface soils. Geochimica Et Cosmochimica Acta, 2011, 75, 5648-5663.	3.9	64
98	Coupled biotic–abiotic Mn(II) oxidation pathway mediates the formation and structural evolution of biogenic Mn oxides. Geochimica Et Cosmochimica Acta, 2011, 75, 6048-6063.	3.9	191
99	Uranium speciation and stability after reductive immobilization in aquifer sediments. Geochimica Et Cosmochimica Acta, 2011, 75, 6497-6510.	3.9	112
100	Trace Metals as Biomarkers for Eumelanin Pigment in the Fossil Record. Science, 2011, 333, 1622-1626.	12.6	147
101	A Bacterium That Can Grow by Using Arsenic Instead of Phosphorus. Science, 2011, 332, 1163-1166.	12.6	422
102	The MicroAnalysis Toolkit: X-ray Fluorescence Image Processing Software. AIP Conference Proceedings, 2011, , .	0.4	112
103	Discontinuities in the human bone–PDL–cementum complex. Biomaterials, 2011, 32, 7106-7117.	11.4	35
104	Response to Comments on "A Bacterium That Can Grow Using Arsenic Instead of Phosphorus― Science, 2011, 332, 1149-1149.	12.6	23
105	Synchrotron X-ray analyses demonstrate phosphate-bound gadolinium in skin in nephrogenic systemic fibrosis. British Journal of Dermatology, 2010, 163, 1077-1081.	1.5	59
106	Arsenic Localization, Speciation, and Co-Occurrence with Iron on Rice (<i>Oryza sativa</i> L.) Roots Having Variable Fe Coatings. Environmental Science & Technology, 2010, 44, 8108-8113.	10.0	163
107	Spatial Imaging and Speciation of Lead in the Accumulator Plant <i>Sedum alfredii</i> by Microscopically Focused Synchrotron X-ray Investigation. Environmental Science & Technology, 2010, 44, 5920-5926.	10.0	89
108	Site Specific X-ray Anomalous Dispersion of the Geometrically Frustrated Kagomé Magnet, Herbertsmithite, ZnCu ₃ (OH) ₆ Cl ₂ . Journal of the American Chemical Society, 2010, 132, 16185-16190.	13.7	166

#	Article	IF	CITATIONS
109	Characterization of manganese oxide precipitates from Appalachian coal mine drainage treatment systems. Applied Geochemistry, 2010, 25, 389-399.	3.0	71
110	The Interaction of Bromide Ions with Graphitic Materials. Advanced Materials, 2009, 21, 102-106.	21.0	24
111	A seafloor microbial biome hosted within incipient ferromanganese crusts. Nature Geoscience, 2009, 2, 872-876.	12.9	87
112	Effects of Soluble Cadmium Salts Versus CdSe Quantum Dots on the Growth of Planktonic <i>Pseudomonas aeruginosa</i> . Environmental Science & Technology, 2009, 43, 2589-2594.	10.0	147
113	Tracing Copperâ^'Thiomolybdate Complexes in a Prospective Treatment for Wilson's Disease. Biochemistry, 2009, 48, 891-897.	2.5	70
114	XANES Evidence for Oxidation of Cr(III) to Cr(VI) by Mn-Oxides in a Lateritic Regolith Developed on Serpentinized Ultramafic Rocks of New Caledonia. Environmental Science & Technology, 2009, 43, 7384-7390.	10.0	154
115	Structural characterization of terrestrial microbial Mn oxides from Pinal Creek, AZ. Geochimica Et Cosmochimica Acta, 2009, 73, 889-910.	3.9	112
116	Enzymatic microbial Mn(II) oxidation and Mn biooxide production in the Guaymas Basin deep-sea hydrothermal plume. Geochimica Et Cosmochimica Acta, 2009, 73, 6517-6530.	3.9	85
117	Nonreductive Biomineralization of Uranium(VI) Phosphate Via Microbial Phosphatase Activity in Anaerobic Conditions. Geomicrobiology Journal, 2009, 26, 431-441.	2.0	89
118	Comparison of EXAFS foil spectra from around the world. Journal of Physics: Conference Series, 2009, 190, 012032.	0.4	11
119	Structure of Biogenic Uraninite Produced by <i>Shewanella oneidensis</i> Strain MR-1. Environmental Science & Technology, 2008, 42, 7898-7904.	10.0	119
120	Weathering of the Rio Blanco quartz diorite, Luquillo Mountains, Puerto Rico: Coupling oxidation, dissolution, and fracturing. Geochimica Et Cosmochimica Acta, 2008, 72, 4488-4507.	3.9	204
121	XAS Study of a Metal-Induced Phase Transition by a Microbial Surfactant. Langmuir, 2008, 24, 4999-5002.	3.5	13
122	High Rates of Sulfate Reduction in a Low-Sulfate Hot Spring Microbial Mat Are Driven by a Low Level of Diversity of Sulfate-Respiring Microorganisms. Applied and Environmental Microbiology, 2007, 73, 5218-5226.	3.1	59
123	Indirect Oxidation of Co(II) in the Presence of the Marine Mn(II)-Oxidizing Bacterium Bacillus sp. Strain SG-1. Applied and Environmental Microbiology, 2007, 73, 6905-6909.	3.1	56
124	Uranium Biomineralization as a Result of Bacterial Phosphatase Activity:  Insights from Bacterial Isolates from a Contaminated Subsurface. Environmental Science & Technology, 2007, 41, 5701-5707.	10.0	176
125	Determination of Uranyl Incorporation into Biogenic Manganese Oxides Using X-ray Absorption Spectroscopy and Scattering. Environmental Science & Spectroscopy, 2006, 40, 771-777.	10.0	81
126	Enhanced Exopolymer Production and Chromium Stabilization in Pseudomonas putida Unsaturated Biofilms. Applied and Environmental Microbiology, 2006, 72, 1988-1996.	3.1	200

Sam M Webb

#	Article	IF	CITATIONS
127	Zinc sorption to biogenic hexagonal-birnessite particles within a hydrated bacterial biofilm. Geochimica Et Cosmochimica Acta, 2006, 70, 27-43.	3.9	177
128	EXAFS, XANES and In-Situ SRXRD Characterization of Biogenic Manganese Oxides Produced in Sea Water. Physica Scripta, 2005, , 888.	2.5	20
129	Dopant site selectivity in BaCe0.85M0.15O3-l´ by extended x-ray absorption fine structure. Journal of Applied Physics, 2005, 97, 054101.	2.5	23
130	Evidence for the presence of Mn(III) intermediates in the bacterial oxidation of Mn(II). Proceedings of the United States of America, 2005, 102, 5558-5563.	7.1	287
131	Structural Influences of Sodium and Calcium Ions on the Biogenic Manganese Oxides Produced by the MarineBacillusSp., Strain SG-1. Geomicrobiology Journal, 2005, 22, 181-193.	2.0	56
132	Biotic and abiotic products of Mn(II) oxidation by spores of the marineBacillus sp.strain SG-1. American Mineralogist, 2005, 90, 143-154.	1.9	237
133	Structural characterization of biogenic Mn oxides produced in seawater by the marine bacillus sp. strain SG-1. American Mineralogist, 2005, 90, 1342-1357.	1.9	243
134	SIXPack a Graphical User Interface for XAS Analysis Using IFEFFIT. Physica Scripta, 2005, , 1011.	2.5	872
135	BIOGENIC MANGANESE OXIDES: Properties and Mechanisms of Formation. Annual Review of Earth and Planetary Sciences, 2004, 32, 287-328.	11.0	1,081
136	XAS Speciation of Arsenic in a Hyper-Accumulating Fern. Environmental Science & Technology, 2003, 37, 754-760.	10.0	168
137	Zinc and lead sequestration in an impacted wetland system. Journal of Environmental Management, 2003, 8, 103-112.	1.7	71
138	Quick X-ray absorption spectroscopy for determining metal speciation in environmental samples. Journal of Synchrotron Radiation, 2001, 8, 928-930.	2.4	31
139	An EXAFS study of zinc coordination in microbial cells. Journal of Synchrotron Radiation, 2001, 8, 943-945.	2.4	14
140	Zinc Speciation in a Contaminated Aquatic Environment:Â Characterization of Environmental Particles by Analytical Electron Microscopy. Environmental Science & Technology, 2000, 34, 1926-1933.	10.0	52
141	Fate of Neptunium in an Anaerobic, Ethanogenic Microcosm. Materials Research Society Symposia Proceedings, 1999, 556, 1141.	0.1	5
142	Determination of photochemically available iron in ambient aerosols. Journal of Geophysical Research, 1996, 101, 14441-14449.	3.3	46
143	Photoreduction of iron oxyhydroxides in the presence of important atmospheric organic compounds. Environmental Science & Technology, 1993, 27, 2056-2062.	10.0	169